Advances in Organic Geochemistry 1989
Org. Geochem. Vol. 16, Nos 4–6, pp. 689–701, 1990
Printed in Great Britain

0146-6380/90 $3.00 + 0.00
Pergamon Press plc

Organic geochemistry of a Lower Jurassic synrift lacustrine sequence, Hartford Basin, Connecticut, U.S.A.

MICHAEL A. KRUGE[1], JOHN F. HUBERT[2], DAVID F. BENSLEY[1], JOHN C. CRELLING[1], R. JAY AKES[1] and PAUL E. MERINEY[2]

[1]Department of Geology, Southern Illinois University, Carbondale, IL 62901, U.S.A.
[2]Department of Geology and Geography, University of Massachusetts, Amherst, MA 01003, U.S.A.

(*Received* 25 *August* 1989; *accepted* 23 *April* 1990)

Abstract—Synrift terrestrial strata of the Lower Jurassic East Berlin Formation (Hartford basin, Connecticut, U.S.A.) record cyclical expansion and contraction of major lakes, six of which were deep enough to develop anoxic bottom waters. We have studied one representative lacustrine sequence in detail, sampling a new roadcut near the village of East Berlin. The section examined is 4 m thick, with a gray siltstone at the base, deposited in shallow water, overlain by an organic-rich black shale (deep water), succeeded in turn by another gray siltstone, deposited as the lake waters gradually receded. The upper gray siltstone is chemically distinct from the lower siltstone, as it contains small amounts of corrensite, analcime and gypsum, reflecting the increasing salinity and alkalinity of the contracting lake.

The samples in the center of the black shale unit contain laminae of thermally-altered, yellowish orange-fluorescing, mottled telalginite. The fluorescence properties indicate a peak oil generation maturity level, confirmed by a vitrinite reflectance of 1.13% and a Methylphenanthrene Index of 1.08. The other samples have less organic matter, becoming increasingly lean towards the top and bottom of the sequence.

Samples in the middle of the black shale unit are distinguished by the presence of an homologous series of tricyclic terpanes extending from C_{20} to at least C_{41}, and by the near absence of hopanes and steranes. Moving upsection into the gray siltstone, the samples contain markedly less extractable organic material (EOM) and the concentration of tricyclic terpanes relative to hopanes steadily decreases. In the uppermost sample, hopanes are the predominant terpanes. Moving downsection from the black shale into the lower gray siltstone, EOM and the ratio of tricyclic terpanes also decrease, except in the lowermost samples, which contain terpane distributions like those of the middle part of the black shale. This likely is migrated material, because bitumen fills microfractures and extensive megafractures. The lack of hopanes and steranes in the black shales cannot simply be a maturation effect, as these biomarkers appear in the adjacent beds. Instead, the unusual terpane distributions may indicate a changing depositional environment, documenting the geochemical evolution of the lake. Or, more likely, they may result from fractionation during expulsion of petroleum from these mature source rocks.

Key words—biological markers, tricyclic terpanes, migration of petroleum, alginite, lacustrine depositional environment, rift basins, Jurassic, Connecticut

INTRODUCTION

Numerous synrift basins developed early in Mesozoic time on both sides of the future Atlantic, in response to regional extension during breakup of Pangaea (Van Houten, 1977; Lorenz, 1988). Along the eastern margin of North America, the deposits that fill these basins are collectively termed the Newark Supergroup, comprising terrestrial redbeds, basaltic flows and intrusions, and gray-black lacustrine rocks, the latter often organic-rich. There has been renewed interest in the petroleum potential of these basins, particularly those offshore. The onshore Newark basin (northern New Jersey and adjacent Pennsylvania) and Hartford basin (central Connecticut) are well-known geologically and are potential analogs for offshore frontier provinces.

Previous organic geochemical work on the Newark Supergroup has focused primarily on the Newark and Hartford basins, using bulk analytical, chromatographic, petrographic and spectroscopic techniques, to determine petroleum source potential and thermal maturity (Pratt *et al.*, 1986, 1988; Pratt and Burruss, 1988; Spiker *et al.*, 1988; Kotra *et al.*, 1988; Walters and Kotra, 1989; Pratt, 1989). Kruge and others (1989, 1990) have described the organic geochemical similarity of the black shales in each of the six lacustrine sequences in the Lower Jurassic East Berlin Formation of the Hartford basin, noting in particular the presence of a series of extended tricyclic terpanes and the absence of hopanes in each of the black shales. Continuing this work, the present paper focuses on the detailed organic geochemistry and petrology of one full lacustrine sequence to evaluate the effects of a changing depositional environment on the organic matter therein, as well as the effects of oil expulsion from a thermally mature source bed.

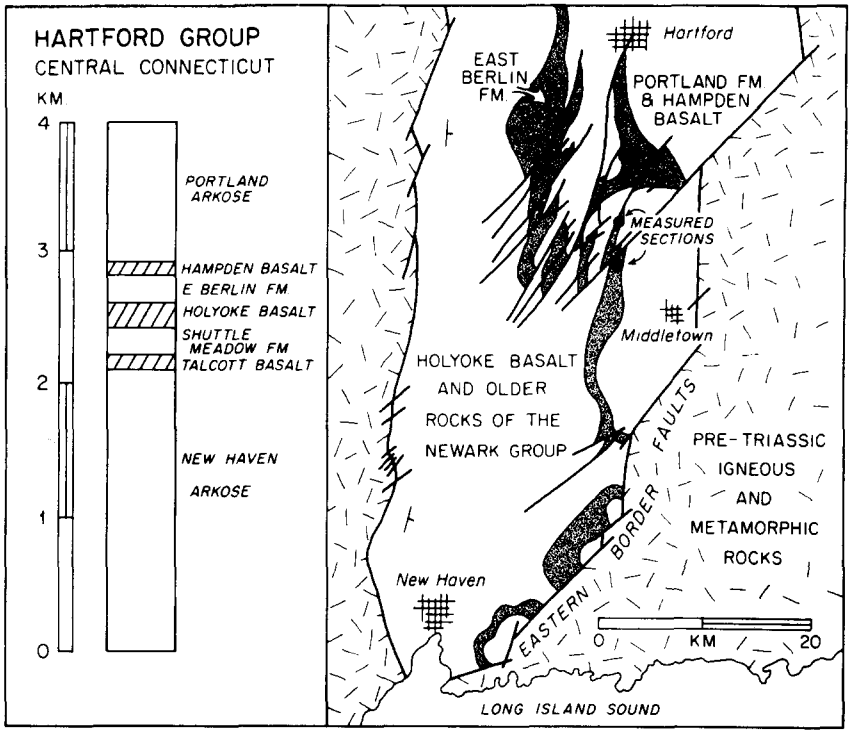

Fig. 1. Stratigraphic column of the Hartford Group in central Connecticut. The location map shows the southern portion of the Hartford basin in central Connecticut. The northern site (●) plotted on the map is the measured section of Fig. 2. The southern site (●) is the "Westfield fish bed".

GEOLOGICAL SETTING

Stratigraphy and sedimentology

The Lower Jurassic East Berlin Formation is a unit of the synrift Hartford Group (Fig. 1), the central Connecticut portion of the Newark Supergroup. In the middle and upper parts of the East Berlin Formation, six lacustrine intervals of 4–8 m of gray siltstone and sandstone and black shale are interbedded with playa and fluvial red mudstone and sandstone (Hubert *et al.*, 1978, 1982; Demicco and Kordesch, 1986; Meriney, 1988). We focus primarily on the deposits of the fourth oldest lake, which record a complete symmetrical sequence, beginning with playa red sandy mudstone and sandstone, overlain by lacustrine deposits of, in stratigraphic order, gray sandstone, gray siltstone, black shale, gray siltstone and gray sandstone (Figs 2 and 3). At the top of the sequence, playa red sandy mudstone and sandstone recur.

The black shale of the fourth lake comprises an interval of 50 cm in thickness (Figs 2 and 3), covering an area of at least 20 by 80 km (Hubert *et al.*, 1976). The lower half of the black shale is laminated with alternating mm-scale layers of dolomite with minor detrital clay and detrital clay/kerogen with minor dolomite. The total organic carbon content of a black shale sample (sample 6), collected 10 cm from the top of the interval, is 2.6%. Throughout the black shale, there are dispersed grains of quartz and feldspar, mm-scale spheroidal groups of authigenic magnesite crystals, and small amounts of authigenic pyrite. Laminae of silt and fine micaceous sandstone are present towards the top of the black shale. Fish scales are occasionally present, especially in the laminated interval. The black shale lacks mudcracks, burrows and evaporite molds.

Gray sandy siltstone below and above the black shale comprises intervals of 125 and 175 cm thick respectively (Figs 2 and 3). The siltstones are micaceous and contain a few horizons of ripple cross-laminated sandstone, cemented by albite and dolomite. There is one horizon rich in rounded clasts of dolomite. Authigenic pyrite occurs throughout the siltstones as disseminated crystals and concentrated in layers. Some siltstone horizons are characterized by complex superimposed mudcracks filled with gray mudstone (Demicco and Kordesh, 1986). In the gray siltstone above the black shale, there are traces of authigenic corrensite and analcime (April 1981), as well as disseminated clumps and crystals of gypsum and mm-size vugs filled with albite and ferroan dolomite. Nodules of dolomite are common in the upper part of the upper gray siltstone, either disseminated or concentrated in layers.

Gray sandstone intervals at the top and bottom of the lacustrine sequence measure 50 and 100 cm, respectively (Fig. 2). The sandstones are mostly plane-bedded, with minor ripple cross-lamination and decimeter-scale planar crossbeds. Authigenic albite overgrowths, ferroan dolomite cement and

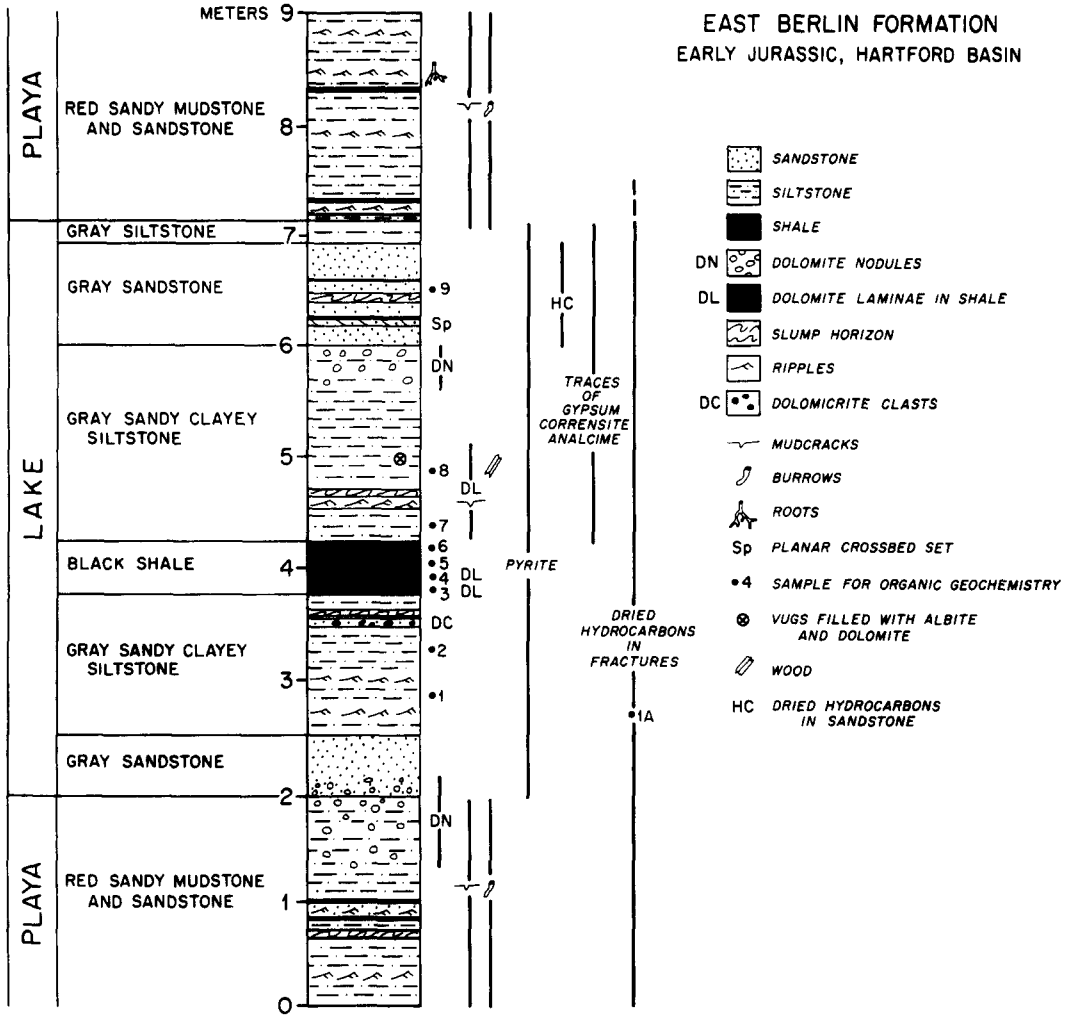

Fig. 2. Stratigraphic section of the fourth oldest lake sequence of the East Berlin Formation. Lithologies and sample numbers (1–9) are given. See Fig. 1 for location.

dried petroleum comprise *ca* 35% (by volume) of the sandstones, indicating cementation was completed before substantial compaction. Albite came first in the diagenetic sequence, then ferroan dolomite, followed by development of secondary porosity due to dissolution of dolomite. Petroleum migrated into secondary pore spaces. The sandstones now have 1–3% porosity.

Red sandy mudstone and sandstone bound the lacustrine sequence above and below. Mudcracks and *Scoyenia* burrows occur throughout the redbeds. *Eubrontes* footprints 30–40 cm in length are found in the gray siltstones and adjacent red mudstones, recording excursions to the lake by these carnivorous dinosaurs which were about 2 m tall and 6 m long.

Paleoenvironmental interpretation

The strata of the fourth lake are part of a sequence of similar units in the East Berlin Formation that occur with a vertical spacing of about 10 m within redbeds of playa and fluvial mudstone and sandstone (Hubert *et al.*, 1976, 1978). The cyclicity is interpreted to be due to increased precipitation controlled by the 23,000 year precession cycle of the earth's axis (Olsen, 1986). The lakes formed during cycles of increased precipitation in an otherwise semi-arid climate (Suchecki *et al.*, 1988).

The interval of gray sandy siltstone below the black shale records the expansion of the lake. At this time, the lake was shallow and wind-driven waves swept the lake floor, spreading ripples and laminae of sand and silt. The black shale accumulated in a perennial oligomictic lake, whose stable thermal stratification was rarely completely overturned. The lake deepened eastward, filling a closed depression created by basin subsidence along the listric normal fault on the east side of the valley. The lake covered at least 1600 km^2, which suggests depths of at least a few tens of meters. The dolomite laminae and authigenic albite, gypsum, pyrite, dolomite, correnside and magnesite in the lacustrine strata indicate that the lake was alkaline, withs substantial amounts of dissolved bicarbonate, calcium, magnesium, sodium and sulfate. Absence of bedded evaporites suggest that it was not a truly saline lake.

Table 1. Organic petrography

Sample No.	1	3	4	5	8
Alginite	0	4	14	1	0
Liptodetrinite	<1	5	2	7	<1
Vitrinite	1	4	<1	<1	2
Inertinite	2	8	9	6	3
Total	3	21	25	14	5
R_o	—	1.13	—	—	—

Compositional data reported as volume percent of total rock. Vitrinite reflectance (R_o) as percent. See text for details of petrographic methods.

The alternating clay and dolomite laminae are probably varves (Hubert *et al.*, 1976). During the dry season, a Mg-calcite precursor of the dolomite precipitated from the epilimnion of the thermally stratified lake, perhaps associated with algal blooms. During the wet season, flooded streams carried detrital clay into the lake, which later settled from suspension. Oxygen-poor bottom waters precluded destruction of the laminations by burrowing infauna, but permitted preservation of the fish fossils. The laminae are best developed in the lower part of the black shale, when the lake was deepest and had its most stable thermal stratification. The number of laminae imply that the lake lasted for hundreds, or perhaps, thousands of years.

The shallowing and desiccation of the lake are recorded by the upper interval of gray sandy siltstone. Horizons of mudcracks record wide lateral fluctuations in the shoreline of the shallow lake. As the lake contracted, periods of elevated salinity were common, as shown by: (1) numerous layers of dolomicrite; (2) rare laminae of gypsum precipitated from the lake; (3) mm-scale vugs lined by dolomite overlain by gypsum; (4) small amounts of authigenic corrensite and magnesite; (5) traces of analcime; and (6) scattered crystals and clumps of gypsum.

EXPERIMENTAL

Black shale, gray siltstone, fracture-filling bitumen and oil-stained sandstone samples from the deposits of the fourth oldest lake (East Berlin Formation) were collected from a fresh roadcut near the intersection of Connecticut state highway 9 and U.S. interstate highway 91, *ca* 2 km east of the village of East Berlin (Fig. 1). Samples were pulverized and extracted (CH_2Cl_2) in a Soxhlet apparatus. The dried extracts were separated by liquid chromatography into "saturate", "aromatic", "polar 1" and "polar 2" fractions (silica gel, activated at 300°C for 3 h, with n-C_6H_{14}, 9:1 n-C_6H_{14}:CH_2Cl_2, CH_2Cl_2 and 1:1 CH_2Cl_2:CH_3OH as the respective eluants). The saturate and aromatic fractions were analyzed by gas chromatography/mass spectrometry (GC/MS) with a 25 m OV-1 column (0.2 mm i.d., film thickness 0.33 μm), initially held at 100°C for 10 min, then programmed from 100 to 300°C at 3°C min^{-1}, then held at 300°C for 18 min, using a Hewlett–Packard 5890A GC coupled to an HP 5970B Mass Selective Detector run in selected ion monitoring mode. Peak area quantitation was done on mass chromatograms of the ions given in Table 2.

Petrographic analysis was undertaken using both white and blue light illumination. The volume of organic matter in the rocks was determined using whole rock petrographic preparations. Maceral distributions were determined on kerogen concentrates isolated by standard HCl and HF digestion procedures. These data were then recalculated as volume percentages of whole rock. Reflectance measurements were undertaken on whole rock samples using average reflectance, without the use of a polarizing filter.

ORGANIC PETROLOGIC RESULTS

The eight shales and siltstones (samples 1–8, Fig. 2) were examined qualitatively and samples 1, 3, 4, 5 and 8 were chosen for quantitative petrography (Table 1). Black shale samples 3, 4 and 5 had an abundance of organic material, consisting chiefly of thermally-altered telalginite, characterized by a mottled granular texture under blue light [Fig. 4(a)], and liptodetrinite, disseminated organic material lacking distinctive morphology but possessing fluorescent properties. The telaginite fluoresced a yellowish orange, as determined by chromaticity analysis, weighted by the blue illuminant. All three samples showed significant bitumen staining of the mineral matter matrix when analyzed under blue light. Bitumen-stained minerals were considered to be inorganic rather than organic matter for purposes of point counting. Vitrinite was relatively rare in all samples. It is most abundant in sample 3, of which it comprises only 4% by volume. Inertinite forms about 7–8% of the black shales. The gray siltstone samples have considerably less solid organic matter, becoming progressively leaner towards the bottom- and topmost samples. However, bitumen staining is evident in all samples to some extent. Sample 1, although lacking in distinctive maceral assemblages, has a microfracture network filled by fluorescing material consisting of exudatinite or migrated petroleum [Fig. 4(b)].

It should be noted that an abundance of angular to rounded fluorescing masses about 30–60 μm in diameter were found in the central portion of the black shale [Fig. 4(c)]. While these appeared to resemble some forms of telalginite with radial morphology, thin-section petrographic evidence indicates that they are radiating clusters of magnesite crystals, confirmed by the fact that magnesium is the only major element detectable by EDAX analysis of these particles on a scanning electron microscope.

A total of 75 reflectance measurements were made on sample 3. Two populations were apparent: one with a mean reflectance of 1.13% and the other, 1.43%, corresponding to vitrinite and semifusinite, respectively.

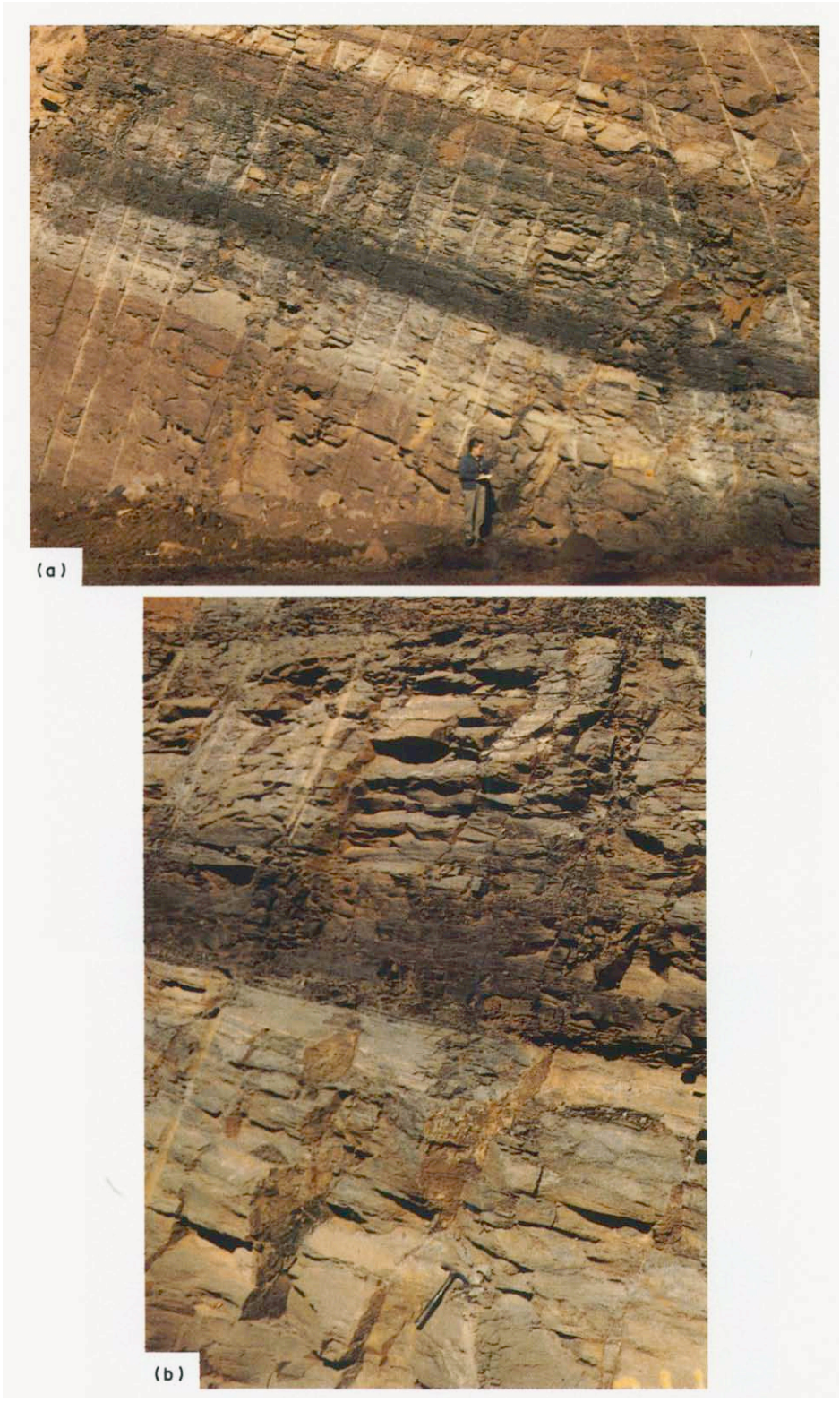

Fig. 3. Photographs of the fourth lake sequence outcrop. See Fig. 1 for location. (a) The full lacustrine sequence. (b) Details of the black shale and the lower gray siltstone, showing oil-stained fractures, the elongated dark vertical zones to the left of the rock hammer in the lower portion of the photograph.

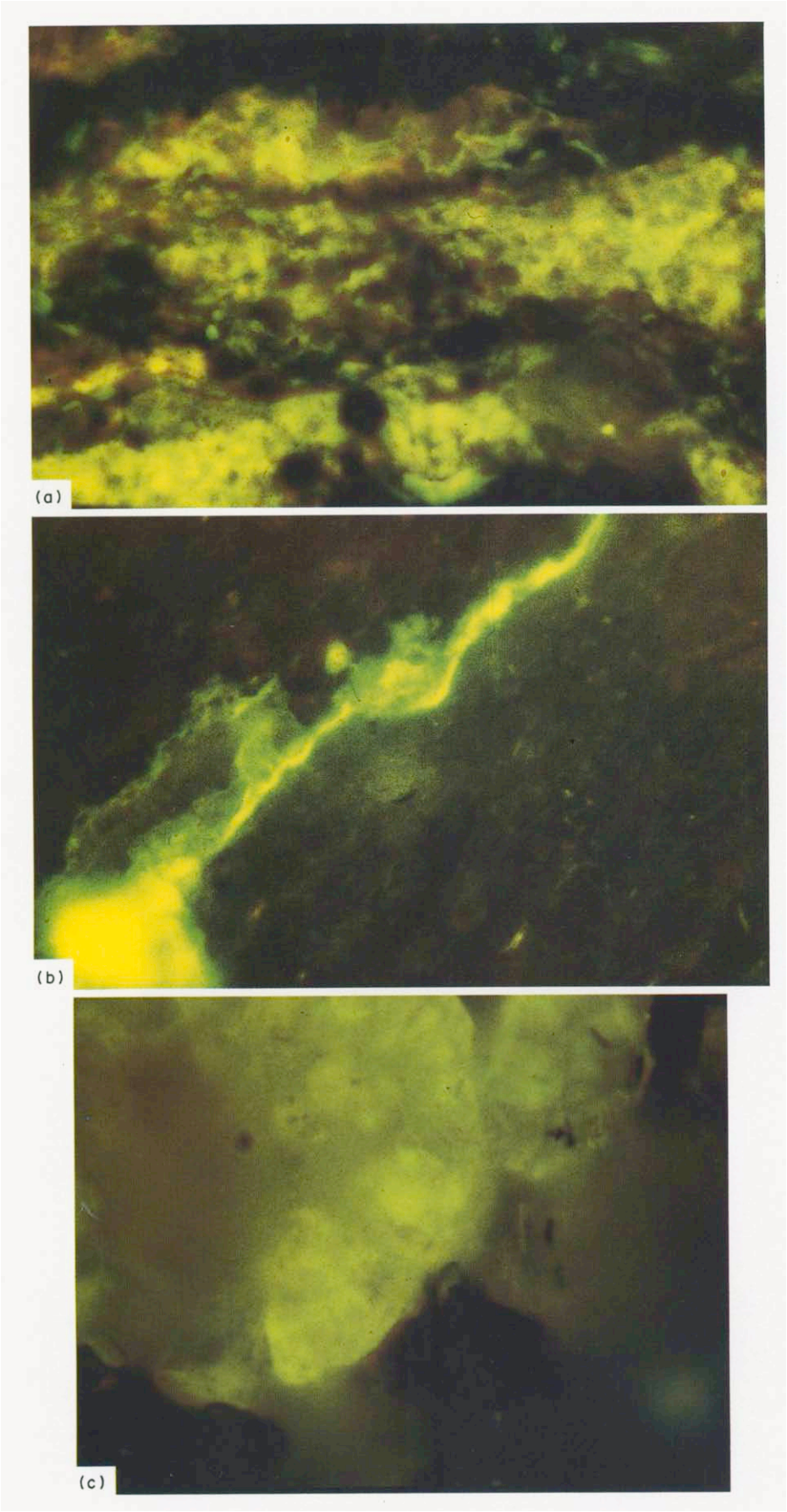

Fig. 4

Table 2. Geochemical results

Sample	1A	1	2	3	4	5	6	7	8	9
EOM‰	10.0	5.0	1.1	1.6	4.1	3.9	1.0	1.0	0.1	0.2
S/P	10.5	5.8	3.1	2.0	3.3	4.1	3.2	1.3	ND	ND
PR/n-C_{17}	1.17	0.56	0.77	0.38	0.42	0.40	0.50	0.91	0.71	0.79
PR/PH	0.76	1.34	1.38	1.35	1.30	1.32	1.39	1.38	0.98	1.14
ST$\alpha\alpha$	ND	ND	0.40	0.57	ND	ND	0.39	0.46	0.43	0.44
ST$\beta\alpha$	ND	ND	0.53	0.35	ND	ND	0.58	0.48	0.47	0.46
TRC	0.50	0.34	0.20	0.47	0.45	0.48	0.46	0.36	0.20	0.36
T/H	1.00	0.84	0.50	0.74	0.97	1.00	0.78	0.29	0.13	0.14
MPI	0.37	1.16	1.09	1.09	—	1.07	—	1.22	—	—

See Fig. 2 for sample lithology. ND, not determinable; —, no data; EOM‰, mg extractable organic matter per g rock; S/P, ratio of saturate to combined polar LC fractions; PR/n-C_{17}, pristane/n-C_{17} ratio (data from peak area quantitation, m/z 99 mass chromatograms); PR/PH, pristane/phytane ratio (m/z 99); ST$\alpha\alpha$, C_{29} 5α,14α,17α 20S/(20S + 20R) ratio (m/z 217); ST$\beta\alpha$, C_{29} 5α,14β,17β/(5α,14β,17β + 5α,14α,17α) ratio (m/z 217); TRC, $C_{21}/(C_{21}+C_{23})$ tricyclic terpane ratio (m/z 191); T/H, C_{23} tricyclic/(C_{23} tricyclic + C_{30} hopane) ratio (m/z 191); MPI, Methylphenanthrene Index (Radke and Welte, 1983) (m/z 178 for phenanthrene and 192 for methylphenanthrenes).

ORGANIC GEOCHEMICAL RESULTS

Extractable organic matter (EOM) concentrations vary considerably among the samples (Table 2). Samples 4 and 5, from the middle of the black shale unit, yielded ≈4 mg EOM/g rock. EOM concentrations drop to ≈1 mg/g rock at the black shale/gray siltstone contacts. The uppermost gray siltstone and oil-stained sandstone have even lower EOM contents. Samples 1 (the microfractured lowermost gray siltstone) and 1A (bitumen collected from a megafracture in the lower gray siltstone) have high EOM concentrations (5 and 10 mg/g rock).

The ratio of the saturate to the combined polar fractions ("S/P") varies sympathetically with the EOM concentrations (Table 2). Generally, the S/P ratio is highest in the lowermost gray siltstone, megafracture bitumen, and black shale. It is lower in samples from the black shale/gray siltstone contact. EOM yields from the uppermost gray siltstone and sandstone were too low for reliable S/P determinations.

The distributions of n-alkanes are nearly identical in samples 2–7, the four black shale samples and the two gray siltstone samples immediately above and below the black shale (Figs 2 and 5). The n-alkanes are detectable up to at least C_{35}, with maxima at C_{19} or C_{20}. A slight odd carbon number predominance in the C_{28} to C_{35} range is seen in samples 2, 6 and 7. The n-alkanes in sample 1, the lowermost gray siltstone, are relatively depleted in the lower carbon numbers, showing a maximum at C_{25} (Fig. 5). Sample 8, the uppermost gray siltstone, is also distinctive, showing maxima at C_{19} and C_{22} and a pronounced odd carbon number predominance in the C_{28} to C_{32} range. Samples 1 and 8 are also relatively depleted in n-alkanes as a whole, as evidenced by the raised chromatographic baseline (Fig. 5). Sample 9, the sandstone extract, is severely depleted in n-alkanes larger than C_{20}. Sample 1A, the magafracture-filling bitumen from the lower gray siltstone, shows an opposite effect: depletion in n-alkanes below C_{25}.

The distribution of the isoprenoids relative to normal alkanes, exemplified by the pristane/n-C_{17} ratio, varies widely among the samples (Table 2). This ratio varies from 0.38 to 0.50 in the black shales, but is much higher in the gray siltstones, varying from 0.56 to 0.91. It is also high (0.79) in the oil-stained sandstone and even higher still (1.17) in the megafracture-filling butumen. The pristane/phytane ratio is more constant among the samples (Table 2), varying only from 1.30 to 1.39 in samples 1–7. These ratios in the uppermost gray siltstone (0.98) and the sandstone (1.14) are slightly lower. The megafracture-filling bitumen is again anomalous, with a vary low ratio of 0.76, possibly due to preferential evaporation of pristane.

Carotanes were detected in the black shales, gray siltstones and fracture-filling bitumen. They are characterized by strong m/z 83 and 123 fragments (Jiang and Fowler, 1986), with β-carotane eluting just after n-C_{37} and γ-carotane, just after n-C_{36}, under the GC conditions employed in this study. Where detectable, γ-carotane is present in amounts greatly subordinate to β-carotane. No carotanes were found in the extract of the oil-stained sandstone.

Steranes and aromatic steroids (except for C_{20} and C_{21} triaromatics) are barely detectable in the black shales of the six lacustrine sequences of the East Berlin Formation (Kruge *et al.*, 1990). However, we now report that steranes are present in the gray siltstone, less than 1 m above the black shale of the fourth lake (Fig. 6). Among the steranes in the gray siltstone, C_{29} homologues predominate and the C_{28}

Fig. 4. Photomicrographs of the East Berlin samples, with blue light illumination. (a) Laminae of thermally-degraded telalginite (sample 4). Photograph is *ca* 56 μm across. (b) Bitumen in microfractures (sample 1). Photograph is *ca* 72 μm across. (c) Radial clusters of fluorescing magnesite crystals (sample 4). Photograph is *ca* 72 μm across.

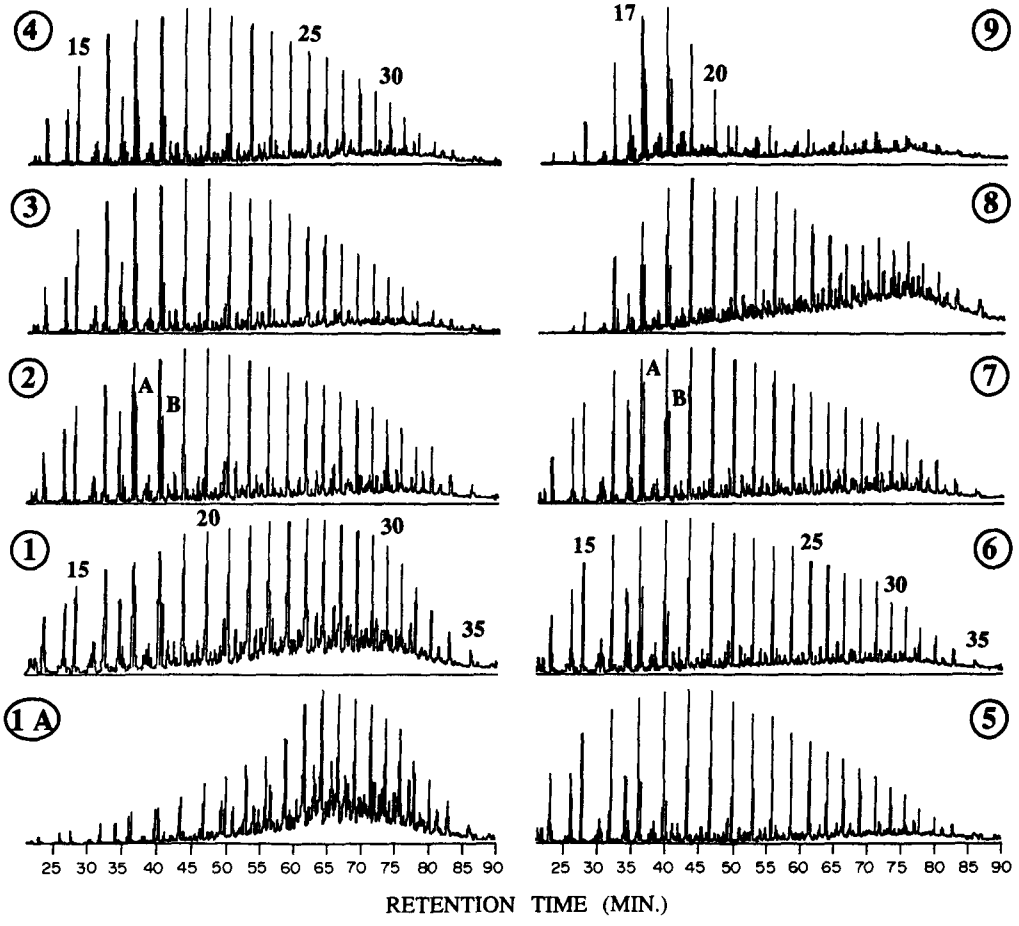

Fig. 5. Distribution of normal and isoprenoid alkanes in the sample suite, as shown on *m/z* 99 mass chromatograms. Sample numbers are circled. Numbers over peaks are *n*-alkane carbon numbers. "A" is pristane, "B" is phytane.

are the least abundant. Diasteranes are prominent. Judging from its *m/z* 217 mass chromatogram, sample 6, from the uppermost part of the black shale, appears transitional from the middle of the black shale to the overlying gray siltstone (Fig. 6). Steranes are present, but weak in sample 3 (lower part of the black shale) and sample 2 (lower gray siltstone), much like sample 6. Steranes are barely discernible in samples 1 and 1A, similar to the innermost black shales. Triaromatic steriods in the C_{26}-C_{28} range are also present in the upper gray siltstone, but the monoaromatic are not. In the upper gray siltstone, there is a higher concentration of dibenzothiophene relative to C_4-substituted naphthalenes than there is in the black shale, as seen on *m/z* 184 mass chromatograms of the aromatic fraction.

The *m/z* 191 mass chromatograms of the saturate fractions document some of the most interesting features of the East Berlin samples. The black shales in each of the six lacustrine sequences contain a series of extended tricyclic terpanes from C_{20} to at least C_{41} (Kruge *et al.*, 1989, 1990). Figure 7 shows a representative terpane distribution (sample 6, the upper part of the black shale of the fourth lake). The C_{19} tricyclic terpane is present in low concentrations, if at all. Note particularly the C_{30} and higher homologues, which are in relative high abundance. The high molecular weight tricyclic terpanes have been detected previously in a terpane concentrate and by metastable ion GCMS analysis (Moldowan *et al.*, 1983), but in the East Berlin black shales, these terpanes can be seen by normal GCMS analysis of the standard saturate fraction. The terpane elution pattern reported by Moldowan and others (1983) is identical with that seen in the East Berlin samples, confirming the peak identifications (Kruge *et al.*, 1990). Hopanes are also present in sample 6, but in subordinate amounts (Fig. 7).

In addition to the black shales, we now report that the extended tricyclic terpane series is also present in the gray siltstones, particularly in those below the black shale (Fig. 8). They are especially strong in sample 1A, the megafracture-filling bitumen. However, moving up into the gray siltstone above the black shale, hopanes become the dominant terpanes, as they are in sample 9, the oil-stained sandstone. The sequence moving from sample 5 up to sample 8 illustrates a gradual transition from virtually all tricyclics to nearly all hopanes (Fig. 8), with the C_{23} tricylic/(C_{23} tricyclic + C_{30} hopane) ratio ("T/H")

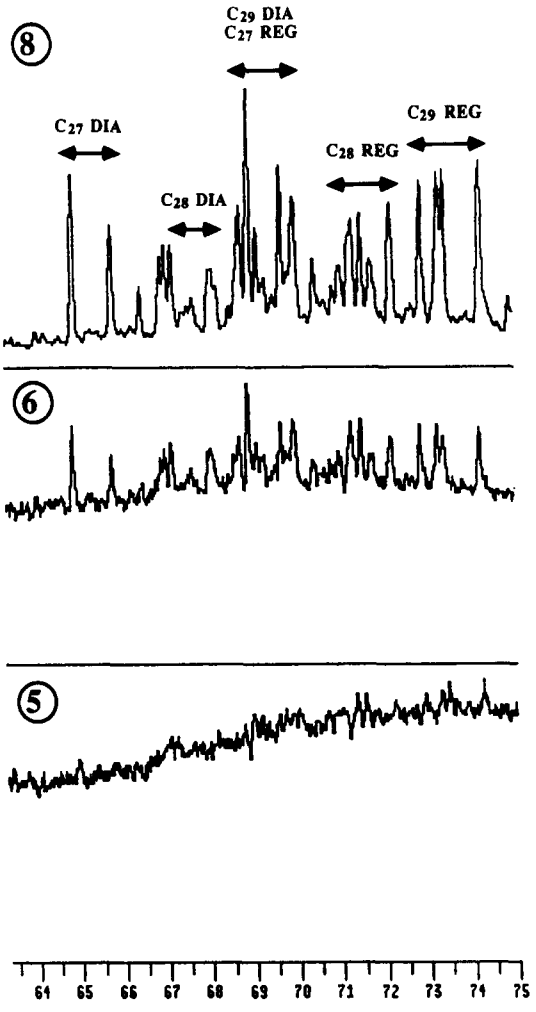

Fig. 6. Representative m/z 217 mass chromatograms showing regular sterane (REG) and diasterane (DIA) distributions. Sample numbers are circled.

decreasing from 1.00 to 0.13 (Table 2). It appears that the sequence from sample 4 down to sample 2 illustrates a similar, but not as complete, increase in hopane concentration, as the T/H ratio drops from 0.97 to 0.50. But, sample 1, with its microfracture porosity, and sample 1A, the bitumen from a megafracture, show a lack of hopanes reminiscent of the black shales.

The distribution of tricyclic terpanes is not identical in all samples. For example, the C_{21} and C_{23} homologues are of approximately the same concentration in the black shales and in the fracture-filling bitumen, but C_{23} dominates in the gray siltstones (Fig. 8), as expressed by the $C_{21}/(C_{21}+C_{23})$ ratio ("TRC") in Table 2.

The use of standard biomarker maturity parameters is problematic in the East Berlin case. The sterane ratios, C_{29} 5α,14α,17α 20S/(20S + 20R) ("STαα") and the C_{29} 5α,14β,17β/(5α,14β,17β + 5α,14α,17α) ("STβα"), were not determinable for samples 1, 1A, 4, and 5, because of the extremely low concentrations of steranes (Table 2, Fig. 6). STαα ratios were calculated for the remaining samples. They are anomalously low, but are fairly consistent, varying from 0.39 to 0.46, except for a black shale (sample 3), which has a STαα ratio of 0.57, but based on very low concentrations of steranes. STβα values vary only from 0.46 to 0.48 in the upper gray siltstone and sandstone, where relative sterane concentrations are high, but vary widely (0.35 to 0.58) in the black shale and lower gray siltstone, where steranes are weak (Table 2). Only the C_{20} and C_{21} triaromatic steroids are found on the m/z 231 mass chromatograms of the black shales. Thus the ratio of $C_{20}+C_{21}$ to total triaromatic steroids is at its maximum value of 1.0 for these samples. C_{26}–C_{28} triaromatic steroids are found in low concentration in the gray siltstones, with the triaromatic steroid ratio reaching a minimum of 0.4 in sample 7. No monoaromatic steroids were detected on the m/z mass chromatograms of any sample, so the maturity parameter employing the ratio of tri- to monoaromatic steroids must be assumed to be at its maximum value throughout the sequence. The Methylphenanthrene Indices (MPI) are consistently high for most of the samples, varying from 1.07 to 1.22 (Table 2), with the exception of sample 1A, which has an MPI of 0.37, due to apparent depletion of 2- and 3-methylphenanthrenes. The MPI values are in accord with the vitrinite reflectance value of 1.13% R_o, determined on sample 3, confirming a peak oil generation maturity level for the section (Kruge *et al.*, 1990).

DISCUSSION

It is apparent from sedimentologic, petrographic, and geochemical criteria that the ten samples comprise four groups: (1) the center of the black shale, (2) the upper gray siltstone and sandstone, (3) the "transitional" samples; and (4) the "fracture" samples. The center of the black shale (samples 4 and 5) has ample telalginite, EOM, and saturated hydrocarbons, with well-developed extended tricyclic terpane series and practically no hopanes and steroids. The upper gray siltstone and sandstone (samples 8 and 9) are very lean in both kerogen and EOM. They have hopanes and steroids, but are poor in tricyclic terpanes. They show moderate to severe depletion of high molecular weight *n*-alkanes. The "transitional" samples (2, 3, 6 and 7), collected near the black shale/gray siltstone contacts, show a blend of the characteristics of the first two groups. Samples 3 and 6 are more similar to the center of the black shale than are samples 2 and 7. The "fracture" samples comprise sample 1, with its bitumen-filled microfracture network [Fig. 4(b)] and sample 1A, the bitumen filling a megafracture. They chemically resemble the black shales, except for the depletion of lower molecular weight alkanes in sample 1A. Samples 1 and 1A are gray siltstones, lithologically and petrographically unlike the black shale samples 4 and 5, strongly suggesting that their fracture-filling bitumen is migrated material,

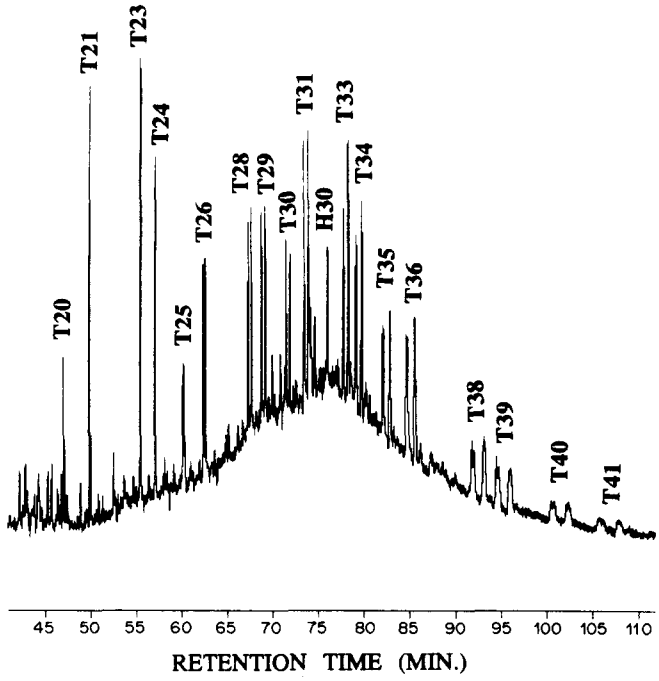

Fig. 7. Distribution of extended tricyclic terpanes in a black shale sample (sample 6), as shown on an *m/z* 191 mass chromatogram. Tricyclic terpane peaks are labelled with a "T" and their carbon number. "H30" identifies hopane.

probably sourced from the black shale. Due to its accessible location within a fracture, sample 1A was subject to weathering or other alteration, witnessed by the lower molecular weight alkane and general *n*-alkane depletion (Fig. 5). The sandstone (sample 9), and to a lesser extent, the siltstone below it (sample 8), also exhibit *n*-alkane depletion, probably due to near-surface alteration. The other samples do not seem to have been weathered, as they are intact rocks, freshly sampled from a newly opened roadcut. The black shales in particular are well-indurated. The extracts of these shales are also rich in *n*-alkanes, which would have been preferentially lost had biodegradation occurred (Volkman *et al.*, 1984).

A variety of standard maturity parameters (vitrinite reflectance, the MPI and the distribution of aromatized steroids) are all consistently high, indicating a mid to late oil window maturity for the sample suite. In samples in which steranes are present in detectable quantities, sterane ratios are anomalously low. Sterane ratios have been observed to decrease at elevated maturity levels (Rüllkotter and Marzi, 1989), which may explain this discrepancy.

Mineralogical evidence indicates that the lake at its deepest, that is, during black shale deposition, was alkaline but not extremely saline. Pratt and Burruss (1988) detected β-carotane in immature black shales from the Hartford basin by gas chromatography, and by the use of the more sensitive GCMS technique, trace amounts of β- and γ-carotanes were shown to be present as well in mature black shales (Kruge *et al.*, 1990). The presence of carotanes is considered to be an indicator of a saline environment (Hall and Douglas, 1983), but not a hypersaline one (ten Haven *et al.*, 1988; Fu *et al.*, 1988). Thus, the organic geochemical data are in accord with the mineralogical.

The organic geochemical transition from the middle black shale to the upper gray siltstone may reflect (1) the different signatures of the original kerogens of the two rock types or (2) fractionation of petroleum during expulsion from the mature black shale. This transition also occurs moving downward from the black shale into the lower gray siltstone, but is apparently incomplete, interrupted by the fracture zone. We will discuss principally the changes in the upward transition, because of its completeness.

The obvious differences in lithology from black shale to gray siltstone reflect major changes in depositional environment, as discussed above, namely the contraction of an alkaline lake, with a corresponding increase in lake water salinity, in response to an increasingly arid climate. Organic remains preserved in the lake sediments also reflect the transition: the telalginite of the organic-rich, deep water black shale gives way to the sparse liptodetrinite and vitrinite of the shallow water gray siltstones. In those organic-lean gray siltstone samples that are free of fractures, the small amounts of bitumen generated would perhaps have been unable to migrate and would remain at their point of origin. The bitumens found in these samples could thus conceivably represent the indigenous kerogen. Thus, one interpretation of the biomarker distributions in the black to gray sequence (samples 5–8) is that they simply reflect the changes in the depositional environment and the associated biota. That is, the extended tricyclic terpanes are

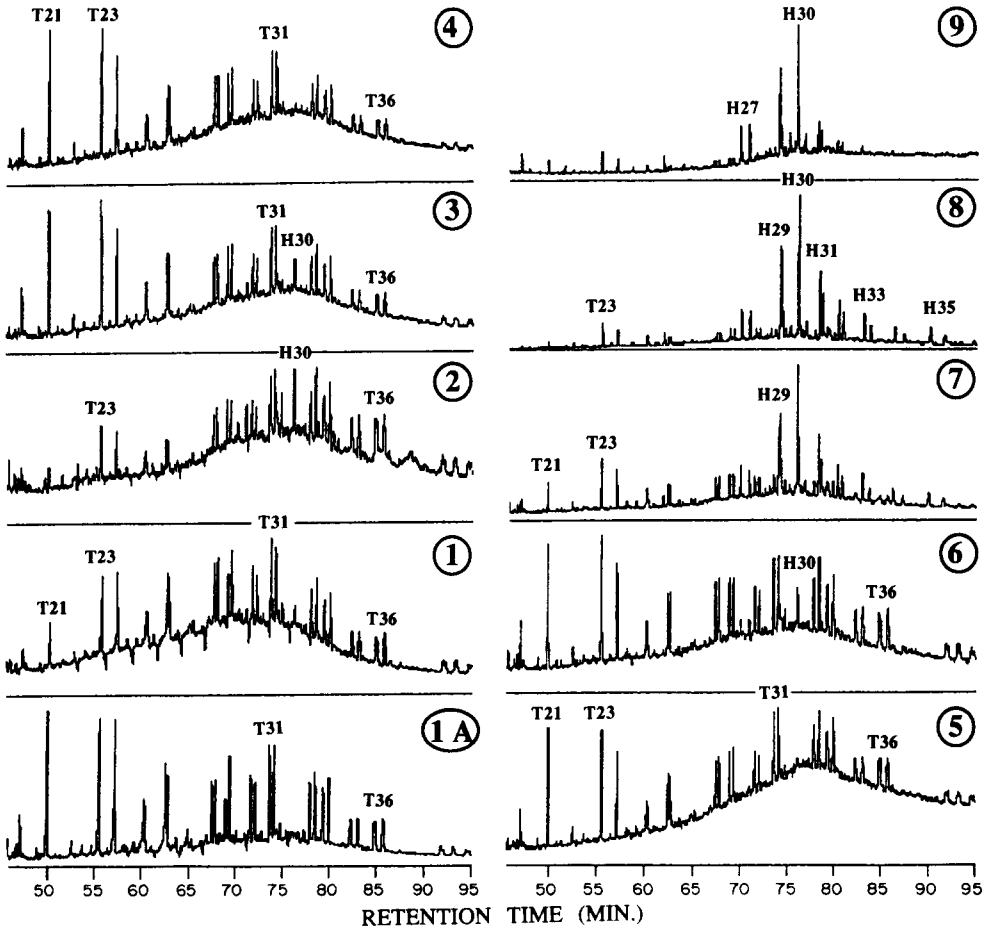

Fig. 8. Distribuiton of tricyclic and pentacyclic terpanes in the sample suite, as shown on *m/z* 191 mass chromatograms. Sample numbers are circled. Selected tricyclic terpane peaks are labelled with a "T" and their carbon number. Selected hopane peaks are labelled with an "H" and their carbon number.

characteristic of the alkaline, anoxic deep lake and the hopanes and steroids reflect the increasing salinity and different organic matter type of the later shallow lake. The higher concentrations of dibenzothiophene relative to C_4-substituted naphthalenes in the upper gray siltstone may reflect the greater sulfur content of the water in the contracting lake.

An alternative (and more likely) explanation for the tricyclic and pentacyclic terpane distributions is the fractionation of migrating hydrocarbons, in a process similar to liquid chromatography in the laboratory. As examples of fractionation, short chain normal alkanes have been shown to migrate more readily than isoprenoid and long chain normal alkanes (Leythaeuser *et al.*, 1984; Leythaeuser and Schwarzkopf, 1986). Laboratory-scale migration simulations conducted using petroleum on an alumina column suggests a more complex picture, with tricyclic terpanes and 5α,14β,17β steranes eluting faster than hopanes and 5α,14α,17α steranes (Fan and Philp, 1987; Jiang *et al.*, 1988). The *m/z* 191 mass chromatograms of the East Berlin black shales resemble the faster eluting fractions from these experiments, whereas those of the upper gray siltstone resemble the slower.

One can envision the mature East Berlin black shale as source rock and the overlying gray siltstone and sandstone as carrier bed or reservoir, within the halo of petroleum radiating from the source. At face value, on comparison with the laboratory work, our geochemical observations appear to show the opposite of the expected effect, i.e. the tricyclic-rich fraction has lingered at the source, while the supposedly slower-migrating hopanes have advanced upwards into the siltstone and sandstone. The explanation may be that, because of the elevated maturity of the source rock ($\approx$1.1% R_o), the tricyclic-rich bitumen present now in the black shale was generated after the occurrence of the initial or main pulse of petroleum expulsion, which emplaced the hopanes in the gray siltstones. In support of this idea, tricyclic terpanes have been generated in the laboratory from petroleum resins and asphaltenes by chemical and pyrolytic degradation (Aquino Neto *et al.*, 1983; Ekweozor, 1984), thus a similar process may occur in nature, cracking the polar components of the residual bitumen in a very mature source rock.

The black shale, being at peak oil generating maturity, has already expelled petroleum. It yields a post-migration residuum upon extraction. Other mature source rock sequences should be studied in similar detail to test this hypothesis. It is unlikely that tricyclic enrichment is due to biodegradation or near-surface alteration, as the rocks in the upper half of the sequence with the strongest evidence for alteration are those with the lowest T/H ratios.

Applying the migration scenario to the gray siltstone below the black shale is less straightforward. There is a gradual decrease in the T/H ratio proceeding from the central black shale (sample 4) downward into the lower transitional samples (samples 3 and 2), symmetrical with that in the sequence moving upward from samples 5 to 7 (Table 2, Fig. 8). However, in the downward sequence, the symmetry ends when the fracture samples are reached and the T/H ratios revert abruptly to high values. In this case, it is likely that we have intersected a direct fracture "pipeline", which allowed freer passage of tricyclic-rich bitumen, during a late stage of expulsion from the black shale source rock at its time of deepest burial, than did the occluded primary pore network within the siltstone. We are now collecting additional samples of oil-stained sandstone and megafracture-filling bitumen as this site for further geochemical study, to gain a clearer understanding of the migration process.

A complex generation and migration history may explain the varying proportions of hopanes and tricyclic terpanes among the East Berlin samples, but it does not account for the occurrence of the extremely long-chain tricyclics. This is most likely the biological marker signature of the particular organic matter preserved in these lacustrine black shales (Kruge *et al.*, 1990). How closely do the extended tricyclic terpanes in the mature bitumen reflect the organic matter of the original black shale? In order to answer this question, we endeavored to obtain samples of less mature East Berlin black shale by sampling an outcrop in Westfield (the "Westfield Fish Bed", Fig. 1) with a reported vitrinite reflectance of 0.5% R_o (Spiker *et al.*, 1988). We call this measurement into question, as we determined the vitrinite reflectance to be 1.13% and found its organic chemistry to closely resemble that of the black shales discussed in this paper. Thus, with its high maturity, it could not be used to determine the terpane content of immature East Berlin black shale. At present, we are sampling other outcrops, continuing to search for less mature samples.

CONCLUSIONS

(1) The Lower Jurassic East Berlin Formation in the synrift Hartford basin contains a symmetrical sequence of gray siltstone to black shale to gray siltstone that records the cyclic expansion and contraction of a large subtropical, alkaline lake. At its deepest, the lake was oligomictic with anoxic bottom waters. As the lake contracted, it became more saline, but not hypersaline.

(2) The organic-rich black shales of this lake preserve mostly thermally-degraded telaginite, lipodetrinite and inertinite, whereas the lean gray siltstones contain sparse liptodetrinite, vitrinite and inertinite.

(3) Optical and molecular maturity parameters confirm a peak oil generation maturity level for the lacustrine sequence.

(4) Black shale extracts contain an unusually extended series of tricyclic terpanes, up to at least C_{41}, with a nearly total exclusion of hopanes and steroids. Gray siltstones and an oil-stained sandstone, although lean in extractable organic matter, show a more typical series of hopanes and steranes, with relatively low tricyclic concentrations. Transitional samples are also present, between the two compositional extremes. Microscopic and megascopic fractures in the siltstones are filled with bitumen very close in terpane composition to the black shales.

(5) The likely cause of the unusually complex biomarker distribution in a lacustrine sequence of only 4 m is the combined effect of the variable nature of the original organic matter types and the phenomenon of fractionation during petroleum migration from a mature source bed. The organic remains incorporated into the black muds on the ancient lake floor produced precursors of the extended tricyclic terpane series. The fractured gray siltstones contain migrated material traceable to the black shales. The other gray siltstones contain small amounts of bitumen either generated from their own sparse kerogen, distinctly different from that in the black shale or, more likely, generated in and expelled from the black shale, perhaps during an early episode, and fractionated during its passage through the siltstone pore network. Other mature source rock sequences should be studied in similar detail to test this hypothesis.

Acknowledgements—We thank J. A. Curiale and J. McEvoy for their thoughtful reviews of the manuscript.

REFERENCES

April R. H. (1981) Trioctahedral smectite and interstratified chlorite/smectite in Jurassic strata of the Connecticut Valley. *Clays Clay Miner.* **29,** 31–39.

Aquino Neto F. R., Trendel J. M., Restle A., Connan J. and Albrecht P. A. (1983) Occurrence and formation of tricyclic and tetracyclic terpanes in sediments and petroleums. In *Advances in Organic Geochemistry 1981* (Edited by Bjorøy M. *et al.*), pp. 659–667. Wiley, Chichester.

Demicco R. V. and Kordesch E. G. (1986) Facies sequences of a semi-arid closed basin: the Lower Jurassic East Berlin Formation of the Hartford basin, New England, U.S.A. *Sedimentology* **33,** 107–118.

Ekweozor C. M. (1984) Tricyclic terpenoid derivatives from chemical degradation reactions of asphaltenes. *Org. Geochem.* **6,** 51–61.

Fan Z. and Philp R. P. (1987) Laboratory biomarker fractionations and implications for migration studies. *Org. Geochem.* **11,** 169–175.

Fu J., Sheng G. and Liu D. (1988) Organic geochemical characteristics of major types of terrestrial petroleum source rocks in China. In *Lacustrine Petroleum Source Rocks* (Edited by Fleet A. J., Kelts K. and Talbot M. R.), pp. 279–289. *Geol. Soc. Spec. Pub. No. 40.*

Hall P. B. and Douglas A. G. (1983) The distribution of cyclic alkanes in two lacustrine deposits. In *Advances in Organic Geochemistry 1981* (Edited by Bjorøy M. *et al.*), pp. 576–587. Wiley, Chichester.

ten Haven H. L., de Leeuw J. W., Sinninghe Damsté J. S., Schenck P. A., Palmer S. E. and Zumberge J. E. (1988) Application of biological markers in the recognition of palaeohypersaline environments. In *Lacustrine Petroleum Source Rocks* (Edited by Fleet A. J., Kelts K. and Talbot M. R.), pp. 123–130. *Geol. Soc. Spec, Pub. No. 40.*

Hubert J. F., Gilchrist J. M. and Reed A. A. (1982) Jurassic redbeds of the Connecticut Valley: (1) Brownstones of the Portland Formation and (2) Playa-playa lake-oligomictic lake model for parts of the East Berlin, Shuttle Meadow, and Portland Formations. In *Guidebook for Field Trips in Connecticut and South-central Massachusetts* (Edited by Joeston R. and Quarrier S.), pp. 1–39. *Connecticut Geological and Natural History Survey Guidebook No. 5.*

Hubert J. F., Reed A. A. and Carey P. J. (1976) Paleogeography of the East Berlin Formation, Newark Group, Connecticut Valley. *Am. J. Sci.* **276,** 1183–1207.

Hubert J. F., Reed A. A., Dowdall W. L. and Gilchrist J. M. (1978) *Guide to the Mesozoic Redbeds of Central Connecticut. Connecticut Geological and Natural History Survey Guidebook No. 4.*

Jiang Z. and Fowler M. G. (1986) Carotenoid-derived alkanes in oils from northwestern China. *Org. Geochem.* **10,** 831–839.

Jiang Z., Philp R. P. and Lewis C. A. (1988) Fractionation of biological markers in crude oils during migration and the effects on correlation and maturation parameters. *Org. Geochem.* **13,** 561–571.

Kotra R. K., Gottfried R. M., Spiker E. C., Romankiw L. A. and Hatcher P. G. (1988) Chemical composition and thermal maturity of kerogen and phytoclasts of the Newark Supergroup in the Hartford basin. In *Studies of the Early Mesozoic Basins of the Eastern United States* (Edited by Froelich A. J. and Robinson G. R.), pp. 68–74. *U.S. Geol. Surv. Bull.* **1776.**

Kruge M. A., Hubert J. F., Akes R. J. and Mereney, P. E. (1989) Extended tricyclic terpanes: molecular markers in Lower Jurassic synrift lacustrine black mudstones of the Hartford basin, Connecticut. *AAPG Bull.* **73,** 375.

Kruge M. A., Hubert J. F., Akes R. J. and Mereney P. E. (1990) Biological markers in Lower Jurassic synrift lacustrine black shales, Hartford basin, Connecticut, USA. *Org. Geochem.* **15,** 281–289.

Leythaeuser D. and Schwarzkopf Th. (1986) The pristane/*n*-heptadecane ratio as an indicator for recognition of hydrocarbon migration effects. *Org. Geochem.* **10,** 191–197.

Leythaeuser D., Mackenzie A., Schaefer R. G. and Bjorøy M. (1984) A novel approach for recognition and quantification of hydrocarbon migration effects in shale-sandstone sequences. *AAPG Bull.* **68,** 196–219.

Lorenz J. C. (1988) *Triassic–Jurassic Rift-Basin Sedimentology: History and Methods.* Van Nostrand Reinhold, New York.

Meriney P. E. (1988) Sedimentology and diagenesis of lacustrine Jurassic sandstones in the Hartford and Deerfield basins, Massachusetts and Connecticut. Unpublished M. S. thesis, University of Massachusetts, Amherst.

Moldowan J. M., Seifert W. K. and Gallegos E. J. (1983) Identification of an extended series of tricyclic terpanes in petroleum. *Geochim. Cosmochim. Acta* **47,** 1531–1534.

Olsen P. E. (1986) A 40-million-year lake record of early Mesozoic orbital climatic forcing. *Science* **234,** 842–848.

Pratt L. M. (1989) Deposition, diagenesis, and maturation of organic matter in rift-basin lacustrine shales of Triassic–Jurassic Newark Supergroup. *AAPG Bull.* **73,** 401.

Pratt L. M. and Burruss R. C. (1988) Evidence for petroleum generation and migration in the Hartford and Newark basins. In *Studies of the Early Mesozoic Basins of the Eastern United States* (Edited by Froelich A. J. and Robinson G. R.), pp. 74–79. *U.S. Geol. Surv. Bull.* **1776.**

Pratt L. M., Shaw C. A. and Burruss R. C. (1988) Thermal histories of the Hartford and Newark basins inferred from maturation indices of organic matter. In *Studies of the Early Mesozoic Basins of the Eastern United States* (Edited by Froelich A. J. and Robinson G. R.), pp. 58–63. *U.S. Geol. Surv. Bull.* **1776.**

Pratt L. M., Vuletich A. K. and Shaw C. A. (1986) *Preliminary Results of Organic Geochemical and Stable Isotope Analysis of Newark Supergroup Rocks in the Hartford and Newark basins, Eastern U.S. U.S. Geol. Surv. Open-File Rept 86–284.*

Radke M. and Welte D. H. (1983) The Methylphenanthrene Index (MPI): a maturity parameter based on aromatic hydrocarbons. In *Advances in Organic Geochemistry 1981* (Edited by Bjorøy M. *et al.*), pp. 504–512. Wiley, Chichester.

Rüllkotter J. and Marzi R. (1989) New aspects to the application of sterane isomerization and steroid aromatisation to petroleum exploration and the reconstruction of geothermal histories of sedimentary basins. *Book of Abstracts*, 197th American Chemical Society National Meeting, Dallas.

Spiker E. C., Kotra R. K., Hatcher P. G., Gottfried R. M., Horan M. F. and Olsen P. E. (1988) Source of kerogen in black shales from the Hartford and Newark basins, eastern United States. In *Studies of the Early Mesozoic Basins of the Eastern United States* (Edited by Froelich A. J. and Robinson G. R.), pp. 63–68. *U.S. Geol. Surv. Bull.* **1776.**

Suchecki R. K., Hubert J. F. and deWet C. C. B. (1988) Isotopic imprint of climate and hydrogeochemistry on terrestrial strata of the Triassic–Jurassic Hartford and Fundy rift basins. *J. Sed. Petrol.* **58,** 801–811.

Van Houten F. B. (1977) Triassic–Liassic deposits of Morocco and eastern North America: comparison. *AAPG Bull.* **61,** 79–99.

Volkman J. K., Alexander R., Kagi R. I., Rowland S. J. and Sheppard P. N. (1984) Biodegradation of aromatic hydrocarbons in crude oils from the Barrow Sub-basin of Western Australia. *Org. Geochem.* **6,** 619–632.

Walters C. C. and Kotra R. K. (1989) Geochemistry of organic matter-rich Mesozoic lacustrine formations of eastern United States. *AAPG Bull.* **73,** 423–424.